Temperature and LET effects on radiation-induced modifications in non-perfect polyethylenes

K. Furtak-Wrona, M. Cornaton, D. Durand, V. Dauvois, J.-L. Roujou, S. Esnouf, M. Ferry

Temperature and LET effects on radiation-induced modifications in non-perfect polyethylenes

K. Furtak-Wrona[1], M. Cornaton[1], D. Durand[1], V. Dauvois[1], J.-L. Roujou[1], S. Esnouf[1] and M. Ferry[1]

[1] Den-Service d'Étude du Comportement des Radionucléides (SECR), CEA, Université Paris-Saclay, Gif-sur-Yvette, France.

Abstract

Regarding the nuclear safety, the potential accumulation of explosive gases during storage, transport and final disposal of Intermediate Level Long Lived Wastes (IL-LLW) has to be well understood and precisely evaluated. In this paper, we have investigated the Linear Energy Transfer (LET) effect that takes into account the different emitters present in the packages, but also the temperature impact in transport safety cases. We have focused our study on polyethylene, as this polymer presents one of the highest hydrogen radiation chemical yield ($G_0(H_2)$), and because of the explosive and inflammable nature of this gas. Chemical defects included in the polymer in the form of carbonyl (C=O) and vinyl (C=C) groups were explored. Depending on the atmosphere of irradiation, they are the main defects formed in polyethylene under irradiation and they are known to be effective energy and radical scavengers. Characterization of the chemical structure of pristine materials has been done. Hydrogen radiation chemical yields were quantified after polymers irradiation. Additionally, the carbon monoxide release was measured for polyethylenes with C=O moieties. Whatever the type of double bonds present in the polymer and whatever the irradiation conditions, hydrogen emission decreases compared to neat materials. Double bonds are effective scavenging groups to which energy is transferred regardless the irradiation nature. Underlying phenomena are explained in this work.

Keywords

Radiation chemical yields; hydrogen; polyethylenes; defects influence; LET effect; irradiation temperature impact

1 Introduction

The Intermediate Level Long Lived Waste (IL-LLW) packages contain technological waste resulting from the maintaining, operating or dismantling phases of nuclear installations and research laboratories. In such containers, polymers can be found in the form of gloves, filters, cables, seals or bottles and so on. During their whole use they have been in the contact with artificial radioactivity, hence they cannot be thrown in garbage as conventional waste at the end of their life. Once placed inside the IL-LLW packages, these polymers are still subjected to the action of γ, β, and α emitters coming from radioactive elements also located in these containers. In contact with the actinides, molecular changes can occur in these materials and cause such modifications as polymer backbone scission or crosslinking, gas emission and formation of new chemical bonds [1-3].

As three kinds of emitters are present in the IL-LLW containers, the LET impact on the gas emission rates has to be understood. The main effect of LET is to exacerbate the heterogeneity of energy deposition and to increase the local concentration of primary radiolytic products. Chang and LaVerne [4] have shown that the radiation chemical yield of hydrogen increases with LET raising. Moreover, these authors have investigated the effect of chemical structure of polymers (polyethylene PE, polypropylene PP, poly(methyl methacrylate) PMMA and polystyrene PS) on the relative change in hydrogen yield as a function of LET. They have found that at low LET, $G(H_2)_{PE} \sim G(H_2)_{PP} \sim 10 \cdot G(H_2)_{PMMA} \sim 100 \cdot G(H_2)_{PS}$. In the case of PMMA and PS, the low yields were assigned to their carbonyl and aromatic side groups, known to be effective radical scavengers [5-10]. When LET increases from 0.02 to 9.5 $MeV \cdot mg^{-1} \cdot cm^2$, hydrogen yields are increasing, but the relative increase depends on the material under study: a factor of about 2 for polyolefins (PE and PP), about 10 for PMMA and about 30 in the case of PS has been observed by the researchers between the lowest and the highest yields.

In France, the IL-LLW containers are designed for a foreseen deep geological disposal. However, before this final step they need to be transported by road. In order to take into account all the probable risk of accident, the French Nuclear Safety Authority requests to take into account an accident with a resulting fire that might last 24 hours. The temperature inside the waste containers can increase in these conditions up to 150 °C. As many reactions are thermally activated, this parameter has already been evaluated.

Hence, Arai *et al*. [11] have shown that during the radiolysis of methane at low dose rate, the hydrogen radiation chemical yield rises together with the temperature from -78 °C to 495 °C. The effect of gamma irradiation temperature on gas production in inert atmosphere was studied on polyethylene by Wu *et al.,* Seguchi, Mitsui *et al.*, Kang *et al.*, and Bowmer *et al.* [12-16]. These

researchers have confirmed in a consistent way that hydrogen emission increases with temperature raising from room temperature up to 300 °C. However, below 150 °C that corresponds to the melting point of polyethylene, the data show two types of behavior depending on the studies. Either hydrogen radiation chemical yield is constant up to a temperature threshold between 60 and 80 °C and then increases, or it increases whenever the irradiation temperature exceeds the room temperature.

Last but not least parameter to take into account in the IL-LLW packages safety is the polymers evolution with the high doses that are encountered in such conditions. When dose is increasing, whatever the atmosphere to be considered, double bonds are formed. Carbonyl groups are the main new bonds created under oxidative atmosphere, whereas vinylene linkages are the main defects formed under inert atmosphere. These two kinds of bonds are known to be effective scavengers. It can be supposed that with the dose increase, the concentration of energy scavengers will increase, and the gas emission will decrease. This is in agreement, at room temperature, with different works on alkanes as on macromolecules [17-19]. To the best of our knowledge, only Williams *et al*. [20] have analyzed the influence of the irradiation temperature on the stabilization of polyethylene by double bonds. They have irradiated a few mixtures of low-density polyethylene and polybutadiene, and have demonstrated that the protective role of double bonds becomes more important when irradiation temperature rises.

In this work, we have studied polyethylenes (PE) with specific defects to evaluate the Linear Energy Transfer (LET) and the temperature effects on the energy and radical migration. We focus in this article on the impact of chemical structure and defects which are present in polymer chain (C=C and C=O groups). These double bonds were chosen because they are representative of main degradation products, and they are effective energy scavengers. In order to determine their ability to decrease the gas emission radiation chemical yields depending on the irradiation conditions, we have examined the effect of their position (in the polymer backbone or as a pendant groups for C=C bonds) and of their concentration (for C=O bonds).

2 Experimental

2.1 Materials

The polymers used in this work were commercially available polyethylenes or materials obtained from the research laboratories. They were “neat” or almost perfect (PE 181900, PE Goodfellow, PE GURa), or contain defects such as carbonyl groups (PE 427780, PE 427772) or C=C double bonds (MB150, EPDMh). Their designations and in some cases their average

molecular weights given by the suppliers are summarized in Table 1. A first part of this article will be dedicated to their characterization prior to irradiation.

Table 1. Characteristics of polyethylene and aliphatic polymers. M_n and M_w are the number average molecular mass and the mass average molar mass, respectively. "-" : absence of value.

	Polymer designation	Supplier	Reference number	Form	M_n (g·mol^{-1})	M_w (g·mol^{-1})
Perfect polyethylenes	PE 181900	Sigma-Aldrich	181900	Pellets	-	125 000
	PE Goodfellow	Goodfellow		Film	-	-
	PE GURa	OBBL[1]		Cut pieces	-	-
PE with C=C defects	MB150	LCPP[2]		Powder	10 900	21 800
	EPDMh	Nordel	2722	Film	36 000 [21]	254 000 [21]
PE with C=O defects	PE 427780	Sigma-Aldrich	427780	Pellets	5 500	15 000
	PE 427772	Sigma-Aldrich	427772	Powder	1 700	4 000

These materials were chosen for the perfection or for the defects they can present. Three neat polyethylenes were considered as references. Methylene based polymers with C=C defects were chosen because of the position of the double bonds: in the backbone or on the side-chain, which is of great interest to understand the preferential paths of migration of energy and radicals. Finally, polyethylenes 427780 and 427772, supposed to be neat ones, were initially chosen because of their different molecular weights. However, after FTIR analysis (see section 3.3), C=O bonds were found in both materials. As this kind of double bond is the main defect formed in polyethylenes under radio-oxidation [25], we found these two polymers of great interest.

2.2 Irradiation conditions

2.2.1 Sample preparation

Each specimen of polymer was placed in glass tube and evacuated by a vacuum line in order to remove oxygen dissolved in the samples. Then, the glass container was filled with pure helium gas under around 700 mbar and sealed. For each sample/irradiation condition couple, two

[1] OBBL: Harris Orthopaedic Biomechanics and Biomaterials Laboratory (Massachusetts General Hospital, Boston, USA).

[2] LCPP: Laboratoire de Chimie et de Procédés de Polymérisation (CNRS - UMR 140, ESCPE Lyon, Villeurbanne, France).

ampoules were prepared, and irradiated at two different and relatively low doses. Sample weights were estimated to obtain, at the end of the irradiation, a final H_2 content of about $1\%_{vol}$.

2.2.2 Gamma irradiations

Gamma irradiations were performed at LABRA (CEA Saclay, France), with a ^{60}Co source. Dosimetry was performed using a UNIDOS PTW dosimeter equipped with a calibration chamber adjusted every two years by the CEA's LNHB laboratory (COFRAC certification): the ionization chamber was placed in air where the samples were put. No electronic correction was made to take into account the electronic density difference between water and polymers. Uncertainties on given doses are less than 6%.

For the irradiations carried out at high temperature, glass containers were placed in a furnace, which was positioned inside the irradiator. Temperature was increased up to the desired one, then the irradiation was started and continued up to the desired dose.

At room temperature, dose rate was equal to 1.04 $kGy \cdot h^{-1}$ and doses of the two glass containers were 49.9 kGy and 99.8 kGy, respectively. At 60-63 °C, 80 °C and 100 °C, dose rate was equal to 1.09 $kGy \cdot h^{-1}$ and the final dose was 26.1 kGy. Irradiations at 120 °C and 150 °C were performed with a dose rate of 1.00 $kGy \cdot h^{-1}$ and a total dose of 24.0 kGy.

2.2.3 Ion irradiations at room temperature

Ions experiment was performed at Grand Accélérateur National d'Ions Lourds (GANIL, Caen, France). The high energy beamline was used due to the need to go through the ampoule glass walls without reducing drastically the energy of the beam reaching the samples placed inside the glass ampoules.

Homogeneous irradiation was ensured by a x,y-scanned beam (surface of about 36 cm^2). The energy loss was calculated with SRIM[3], based on the TRIM[4] code [22]. Irradiation conditions are gathered in Table 2. In order to avoid significant sample heating, fluxes were chosen in order to limit the power deposition on the sample to 0.5 $mW \cdot cm^{-2}$.

Statistical errors for a given sample and for a single beam are low, at most a few percentage. The systematic errors are higher, and are mainly caused by sample thickness and dose estimation, because of the material composition changes. At the highest dose, the systematic error is less than 10%, so the total one on dose has been estimated at about 10%.

[3] Stopping and Range of Ions in Matter.
[4] Transport of Ions in Matter.

Table 2. Irradiation conditions using the high energy beamline of GANIL.

Beam	^{36}Ar
Initial particle energy (MeV·A^{-1})	95
Particle energy at the entrance of the polymer (MeV·A^{-1})	89
Flux (10^8 cm^{-2}.s^{-1})	3.4
Mean LET (MeV·mg^{-1}·cm^2)	2.5
Mean dose rate (kGy·h^{-1})	500
Fluences (10^{11} cm^{-2})	6.7 and 12.5
Doses (kGy)	290 and 570

2.3 Characterizations

2.3.1 Differential Scanning Calorimetry (DSC)

Differential scanning calorimetry (DSC) measurements have been performed to determine melting temperature and crystallinity, two parameters of great influence on the radiation-induced mechanisms [3]. A Netzsch STA 449 Jupiter instrument was employed in inert atmosphere (helium at a flow rate of 60 mL·min^{-1}), with a temperature gradient of 5 K·min^{-1}. Melting temperature (T_m) is defined as the temperature at the maximum of the melting endothermic peak. Area of the melting peak, ΔH_f, was measured and crystallinity, χ_c, was calculated using equation (S1) of the Supplementary Information (along with the crystallinity data).

2.3.2 Fourier transform infrared spectroscopy (FTIR)

Fourier Transform Infrared spectra of the polymers were acquired using a Bruker Vertex 70 spectrometer equipped with a DTGS (Deuterated TriGlycine Sulfate) detector. Spectra were recorded between 4000 and 600 cm^{-1} at a resolution of 2 cm^{-1} and with 64 accumulated scans.

In most cases, samples were analyzed in Attenuated Total Reflectance (ATR mode) with a Specac Golden Gate single reflection diamond accessory. This technique is chosen for its easiness of use, as no sample preparation is needed. Moreover, it gives significant information on the molecular bond nature evolution under irradiation.

To discriminate if the carbonyl bonds are present on impurities or on the polymer backbone in polyethylenes containing C=O bonds (see section 3.3), experiments were realized in transmission mode. In that specific case, about 10 mg of polymer was mixed with 150 mg of KBr and pellets were formed using a laboratory press.

2.3.3 Gas Chromatography coupled with Mass Spectrometry (GC-MS)

Measurements were performed on an Agilent gas chromatography (GC-6890) coupled with a mass spectrometer (MS5973 N). About 1 µL of polyethylene solubilized in dichloromethane was injected in splitless mode. The inlet temperature was at 250 °C. Molecules were separated on a Sigma-Supelco SLB-MS column 30 m × 0.25 mm x 0.25 µm and analyzed with a mass spectrometer equipped with an electron impact source, set at 230 °C. The MS detector operated in scan mode over a mass-range of 50–300 amu.

The oven was stabilized at 40 °C for 5 min, then a temperature gradient of 20 °C·min^{-1} was applied up to 320 °C and finally maintained at 320 °C for 10 min. Helium was used as the carrier gas at a flow rate of 1.5 mL·min^{-1}.

2.3.4 Gas analyses

As irradiation was carried out under inert atmosphere, the form and the thickness of the samples are not critical parameters for ensuring a homogeneous energy deposition. However, in order to minimize the influence of gas diffusion inside the bulk material, no sample was thicker than 2 mm. A simple calculation using Fick's law shows that the elapsed time between the end of irradiation and the beginning of mass spectrometry gas analysis is always much longer than the maximum time necessary for hydrogen to diffuse out of the samples. Then, it can be assumed that there is no residual hydrogen trapped in the material.

Gas analyses were performed using a quantitative gas mass spectrometer Thermo Fischer Scientific MAT-271 [6]. The instantaneous gas emission rate $\frac{1}{d} \cdot \frac{d[H_2]}{dt}$, in mol·J^{-1}, is obtained using equation (1):

$$\frac{1}{d} \cdot \frac{d[H_2]}{dt} = \frac{P_f \cdot \%_{vol} \cdot V_{free}}{R \cdot T \cdot D \cdot m} \quad (1)$$

d is the dose rate in Gy·s^{-1}, $[H_2]$ corresponds to the hydrogen concentration in mol·kg^{-1} measured after irradiation at a given dose D itself expressed in Gy, P_f refers to the total pressure in the glass

ampoule at the end of the irradiation in Pa, $\%_{vol}$ is the gas volume fraction determined by gas mass spectrometry, V_{free} denotes the free volume in the glass ampoule in m^3, R is the gas constant ($R \approx 8.314\ J \cdot mol^{-1} \cdot K^{-1}$), T defines the sample's temperature under irradiation in K, and m is the mass of the irradiated sample in kg. The same equation is used for the determination of carbon monoxide radiation chemical yields.

As irradiation of each sample was in most cases doubled, given gas instantaneous emission rates were calculated as the average of the two measurements, using equation (1). Standard deviation was determined. It was always lower than 10% for hydrogen release and in most cases higher for carbon monoxide. Whatever the irradiation employed at room temperature, radiation chemical yields given are always mean values obtained using two experimental points. For some few points under γ-rays at temperatures higher than ambient one, only one glass ampoule could be irradiated (for all numerical values, see Table S3 of the Supplementary Information). In such case, errors bars given are the mean error bars (in percentage) of the other experimental data: it accounts for 6% for hydrogen release, and 17% for carbon monoxide.

3 Pristine materials characterization

To understand precisely mechanisms that are underlying the radiation protection effect towards unsaturated bonds in non-perfect polyethylenes, nature, position and concentration of the defects have to be known. Precise characterization of pristine polymers is thus necessary.

Infrared analyses were performed to confirm the presence and the nature of the chemical defects of polyethylenes. Thermal analyses were used to evaluate the thermal properties and the crystallinity of the polymers. Crystallinity has been shown to present no direct influence on the hydrogen radiation-chemical yields when saturated aliphatic polymers are irradiated at room temperature [6] that is why they are presented in the Supplementary Information. Nevertheless, this parameter gives an idea of the samples' structural order. Moreover, as the physical state of the polymers is a key parameter, especially for irradiations performed at high temperatures, melting temperatures of the materials were determined.

In the case where materials are less well defined, complementary characterizations have been performed. It applies to polyethylenes containing C=O defects, supposed to be neat ones when purchased.

3.1 Perfect polyethylenes

The melting temperatures of the perfect polyethylenes are 132 °C for PE 181900, 133 °C for PE GURa and 134 °C for PE Goodfellow, respectively.

Figure 1 shows the infrared spectra, in the ATR mode, of the perfect polyethylenes under study. PE GURa and PE Goodfellow present infrared spectra equivalent to the one of pure polyethylene [23, 24]. Nevertheless, in the case of PE 181900 purchased from Sigma-Aldrich, two very weak bands, centered at 990 cm^{-1} and at 909 cm^{-1} can be observed. They are characteristic of vinyl CH wagging and CH_2 wagging modes, respectively [25]. Due to their weak intensity, this polymer was classified into the category of the perfect materials.

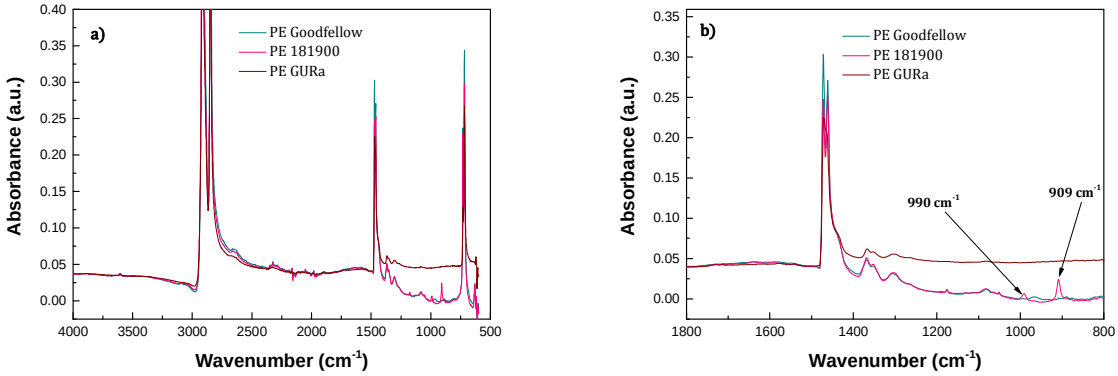

Figure 1. FTIR-ATR spectra of the perfect polyethylenes under study. a) Infrared spectra in the range 4000 – 600 cm^{-1}. b) Zoom in the 1800-800 cm^{-1} area.

3.2 Polyethylenes containing C=C defects

Two polymers containing C=C double bonds were studied in this work. MB150 is a random ethylene/butadiene copolymer, composed of 95% of ethylene and of 5% of butadiene. It can thus be deduced that the vinylenes bonds are located on the backbone of the polymer. On the contrary, EPDMh is a terpolymer containing 75% of ethylene, 19% of propylene and 6% of 1,4-hexadiene [21]. In this case, the vinylenes bonds are located on the polymer side-chain.

The melting temperatures of these methylene based polymers are 118 °C for MB150 and 48 °C for EPDMh, respectively.

ATR-FTIR spectra of the polyethylenes containing C=C double bonds, are compiled in Figure 2. The signature of *trans*-vinylene wagging vibration, at 965 cm^{-1}, can easily be identified. In case of EPDMh, the intense band at 1376 cm^{-1} corresponds to the methylene bending mode of the propylene repetition units [25].

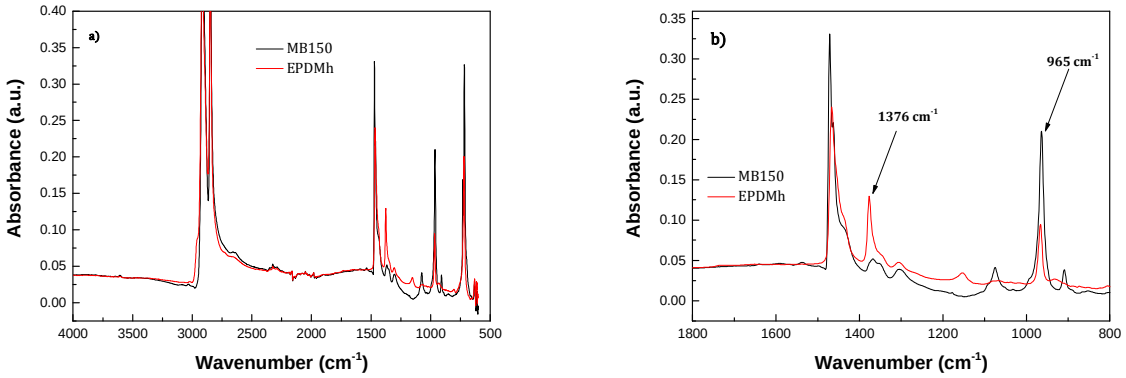

Figure 2. FTIR-ATR spectra of the polyethylenes containing C=C bonds. a) Infrared spectra in the range 4000 – 600 cm^{-1}. b) Zoom in the 1800-800 cm^{-1} area.

3.3 Polyethylenes containing C=O defects

As introduced in section 2.1, an important quantity of carbonyl bonds was evidenced in two polyethylenes.

The melting temperatures of 115 °C was found for PE 427780 and of 107 °C for PE 427772, respectively.

The infrared spectra in the ATR mode are depicted in Figure 3. As indicated just above, the characteristic ketone stretching vibration, at 1720 cm^{-1}, can easily be identified in both polymers [25]. The relative absorbance of this band is two times greater in PE 427772 than in PE 427780. As the intensity of the -CH_2- repetition units are equivalent in both spectra, it can be deduced that the concentration of C=O bands is two times larger in PE 427772 than in PE 427780.

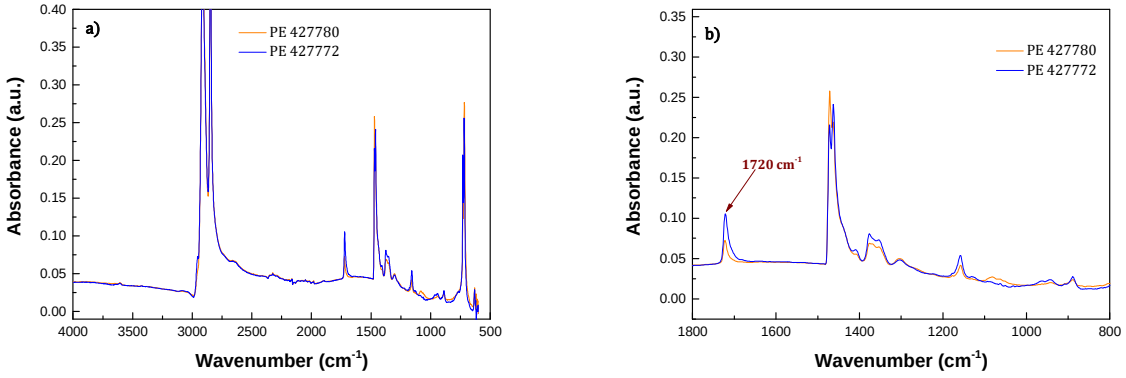

Figure 3. FTIR-ATR spectra of the polyethylenes containing C=O bonds. a) Infrared spectra in the range 4000 – 600 cm^{-1}. b) Zoom in the 1800-800 cm^{-1} area.

In order to obtain more detailed information about polymer chemical compositions, *i.e.* to identify the position of these ketone bonds (in-chain defect and/or impurity), additional characterizations by ^{1}H NMR, ^{13}C NMR and Py-GC-MS have been performed. They are presented in Supplementary Information, because they do not allow to distinguish the presence and/or the position of C=O bonds, maybe because of the detection limits of these analytical methods. It can nevertheless be concluded from these techniques that the two polyethylenes under study are branched ones. To discriminate if the carbonyl bonds are present on impurities or on the polymer backbone, extraction/precipitation of the materials was realized. About 0.1 g was solubilized at 100 °C in 3 mL of toluene; once solubilized, 3 mL of dichloromethane was added to allow precipitation. To separate solubilized and precipitated fractions, centrifugation was realized (13 400 rpm for 5 min). Solid fraction was weighted before and after this manipulation, and at least 90% of the material remains solid, meaning that soluble impurities represent only a weak part of the material. The liquid fraction was analyzed by GC-MS. Even non quantitative, it can be remarked that the number of identified impurities is always smaller in PE 427780 than in PE 427772. Obtained chromatograms and identified chemical compounds are gathered in Supplementary Information.

Potassium bromide pellets containing the different fractions of polymer were prepared and analyzed in transmission mode using FTIR spectroscopy. Spectra of PE 427772 are given on Figure 4. It can be observed that the ketone stretching vibration, at 1720 cm^{-1}, is present in the extract and in the precipitate.

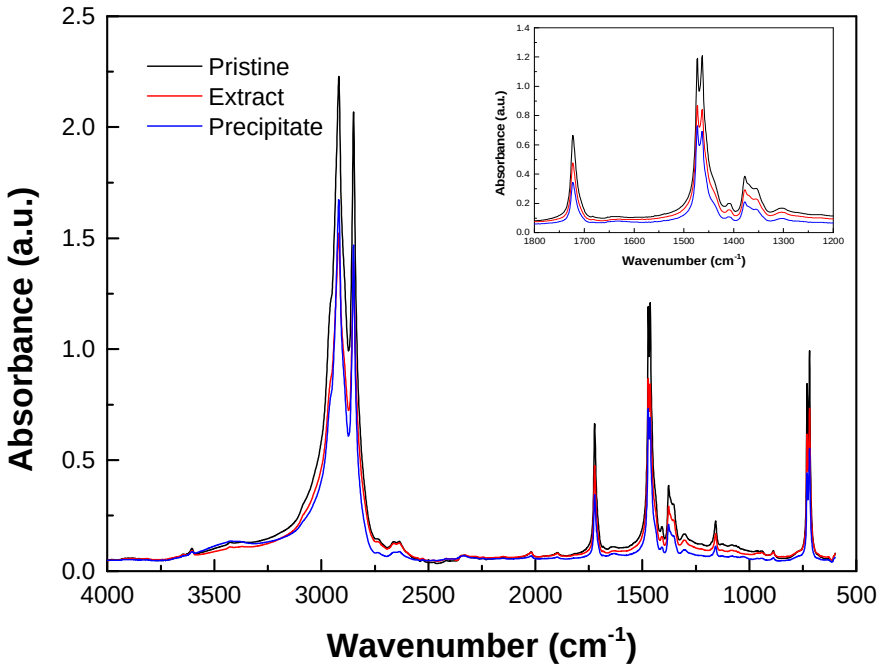

Figure 4. FTIR spectra of the PE 427772 (pristine, soluble part, precipitate). Insert: zoom on the 1800 - 1200 cm^{-1} area.

From the extraction/precipitation and the FTIR experiments, it can be concluded that ketone bonds are present in the backbone and impurities. Nevertheless, as these impurities represent less than 10% of the materials, we will consider in the following that C=O ketone bonds are defects in the backbone and neglect the small proportion present in the impurities. Using infrared spectroscopy in transmission mode and the Beer-Lambert law, we could estimate that $[C=O]_{PE\ 427772} \approx 0.6$ mol·kg^{-1} (*i.e.* about 1.7%$_{wt}$) and $[C=O]_{PE\ 427780} \approx 0.3$ mol·kg^{-1} (*i.e.* about 0.8%$_{wt}$).

Both PE 427772 and PE 427780 are branched polyethylenes with ketone bonds, containing a small quantity of impurities, also containing ketone bonds.

4 Results and discussion

4.1 LET effect

Figure 5 shows the hydrogen radiation chemical yields obtained with the different polymers (numerical data are given in Table S3 of the Supplementary Information). The results obtained by Chang and LaVerne [4] on their polyethylenes was also included as a “line to guide the eye”.

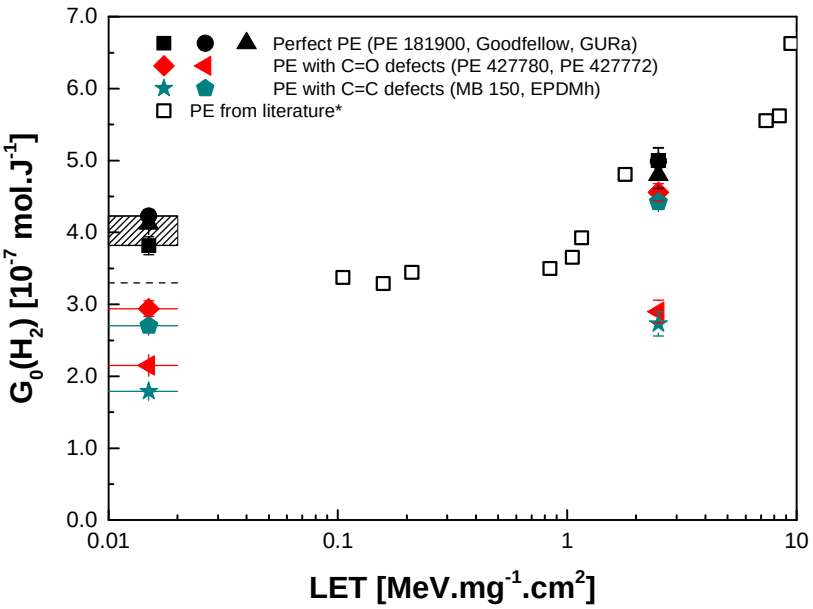

Figure 5. Hydrogen radiation chemical yields as a function of LET for different polyethylenes irradiated under helium atmosphere. Dash line and open squares: results from Chang and LaVerne [4].

It should be emphasized from Figure 5 that polyethylenes Goodfellow and GURa present equivalent hydrogen radiation chemical yields using γ-rays, but $G_0(H_2)$ evolved from PE 181900 is lower. It can probably be attributed to the vinyls bonds protection effect [10, 17], the presence of these double bonds having been evidenced using FTIR spectroscopy (see section 3.1). By using Swift Heavy Ions irradiation (SHI), it is observed that the three neat polyethylenes have equivalent $G_0(H_2)$. It can be deduced from this observation that at higher LET, the hydrogen radiation chemical yields of the three neat polyethylenes are equivalent, so vinyl bonds are no more effective to protect PE. This might at least partially be explained by two facts. The first one is that vinyl bonds are defects that are present only as side-chain effect, and not in the polymeric backbone. In our previous work focused on the effect of ester bonds position effect in methylene containing polymers, we have observed that in-chain defects are substantially more efficient that defects position on side-chains [6]. The second hypothesis comes from the fact that the radiation protection effects of protective bonds are diminished when LET is increasing [3, 4, 26]. It might be concluded that even at low LET, vinyl bonds are less effective than in-chain double bonds to protect polyethylene. Moreover, it seems that the protection effect conferred by these double bonds is lost at lower LET than the one conferred by trans-vinylene bonds.

Figure 5 shows also that at low as at high LET, whatever the kind of double bond (C=O and C=C), the hydrogen radiation yield is decreased when compared with the neat polyethylenes. These two kinds of bonds are known to be effective scavenging groups [9, 10] under low LET irradiation. Here we show that energy transfers towards these defects are efficient whatever the nature of irradiation.

The difference between the two materials containing C=C bonds is the position of the defect in the polymer. The concentration of unsaturations is relatively equivalent in both materials. MB150 presents 5% of unsaturations in the backbone to be compared to 6% in EPDMh [21] on side-chains. The difference in $G_0(H_2)$ is in agreement with our precedent work [6] and with the Partridge's model [18] for energy transfers on polyethylene irradiated using γ-rays. Partridge estimated that about $1/3$ of the excitations are localized on C-H bonds and cannot migrate, whereas $2/3$ are localized on C-C bonds and are allowed to move along the repetition units. In this work, C-H bonds are equivalent to side-chain and C-C bonds correspond obviously to the backbone. By roughly estimating from pure polyethylene the decrease, under γ-rays, due to a scavenger respectively in-chain and side-chain, we obtain:

- In-chain hydrogen radiation chemical yield (decrease of $2/3$ of $G_0(H_2)_{PE\ Goodfellow}$): $1.4 \cdot 10^{-7}$ mol·J^{-1} to be compared to $1.8 \cdot 10^{-7}$ mol·J^{-1} determined for MB150,
- Side-chain hydrogen radiation chemical yield (decrease of $1/3$ of $G_0(H_2)_{PE\ Goodfellow}$): $2.8 \cdot 10^{-7}$ mol·J^{-1} to be compared to $2.7 \cdot 10^{-7}$ mol·J^{-1} determined for EPDMh.

The position and the concentration of the defects have an influence on the radiation chemical yields, which is in agreement with the Partridge's model.

For both MB150 and EPDMh irradiated using SHI, the radiation protection effect conferred by the C=C double bond is decreased compared to irradiations using γ-rays. However, the evolution is not equivalent for both materials, *i.e.* for both defects position. The radiation protection effect is almost lost in case of EPDMh. On the contrary, when defects are in the backbone, radiation protection effect, although less effective than under low LET irradiations, remains active. Regardless of the position of the energy sink, it has been shown by Chang and LaVerne [4] and by Ferry *et al.* [26] that increasing LET induces a loss of radiation protection efficiency, which implies a loss of energy and radical migration. As on side-chains, energy transfers are already drastically reduced compared to in-chains migration under low LET ionizing rays, it can probably be supposed that their protection efficiency will be lost at a LET lower than the one needed to lose the protection induced from in-chains defects. This is exactly what is observed under our SHI irradiations conditions: $G_0(H_2)_{EPDMh} \approx G_0(H_2)_{PE\ Goodfellow}$ whereas $G_0(H_2)_{MB150} < G_0(H_2)_{PE\ Goodfellow}$ under the LET used in this work. Energy and radicals

369 migration are highly efficient in the case of unsaturations on the backbone. It is therefore very
370 probable that under our conditions, only part of the efficiency is lost. It could have been
371 interesting to validate this hypothesis by irradiating MB150 at LET higher than the one of this
372 study.

373 Polyethylenes containing C=O defects are of great interest because their defects are positioned
374 equivalently but their concentration is different: PE 427772 has about twice more C=O defects
375 than PE 427780, numerical values of their concentration being approximations (see section 3.3).
376 Figure 6 presents, as a function of the C=O content, the results obtained for one neat
377 polyethylene (PE Goodfellow has been chosen) without any ketone bond in its structure before
378 irradiation, and the two PE with ketones moieties.

379 From Figure 6, it can be observed for hydrogen release evolution that slopes of the two linear
380 regressions are almost equivalent in the ketone concentration range of this study. The difference
381 observed between γ-rays and SHI irradiations is only due to the difference of energy deposition
382 between the two kinds of irradiations, but the ketone bonds are efficient scavengers in both
383 cases, and in an equivalent proportion.

384 Figure 6 shows also that contrary to the hydrogen evolution, the one of the carbon monoxide
385 release is very dependent on the irradiation nature. Its linear regressions slope is five times
386 more important under γ-rays than under SHI irradiations. This implies that the mechanisms
387 which lead to the formation of these two gases are completely different. The one leading to CO is
388 highly energy and radical transfers dependent. The generally admitted mechanism for CO comes
389 from the decomposition of the ketone bonds by the Norrish type I mechanism [27, 28],
390 presented in Scheme 1. This seems to imply that Norrish type I reaction is influenced by these
391 kind of migration.

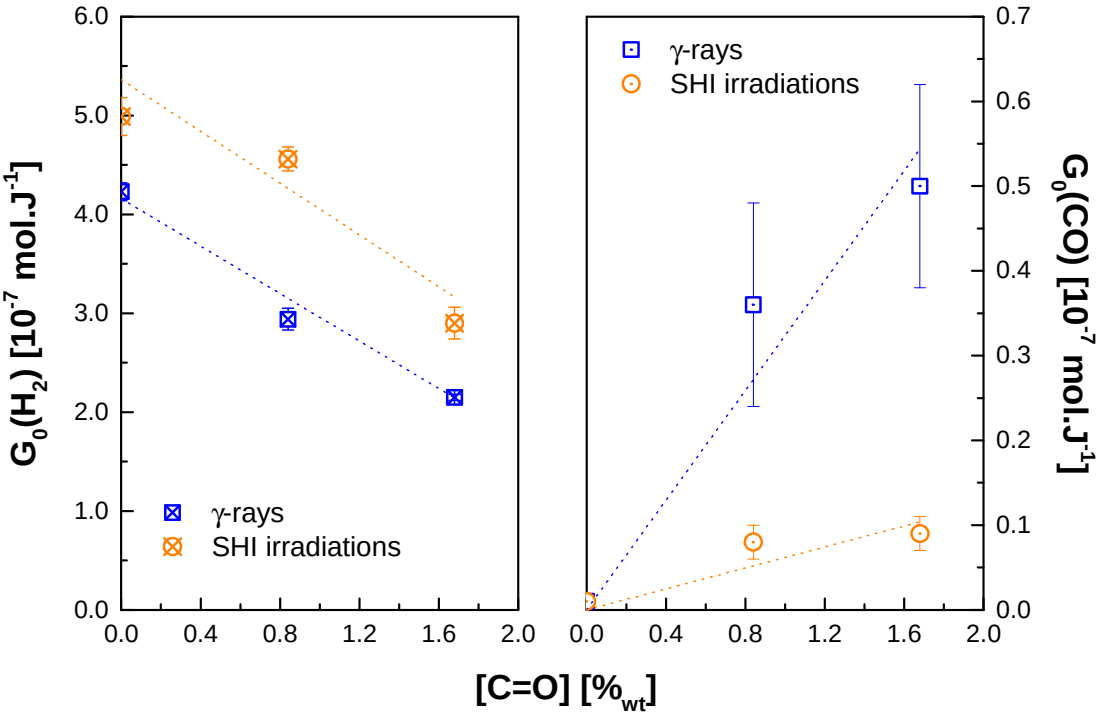

Figure 6. Radiation chemical yields as a function of the initial carbonyl concentration in PE containing C=O bonds. On the left, hydrogen release and on the right, carbon monoxide release. Dot lines: linear regressions.

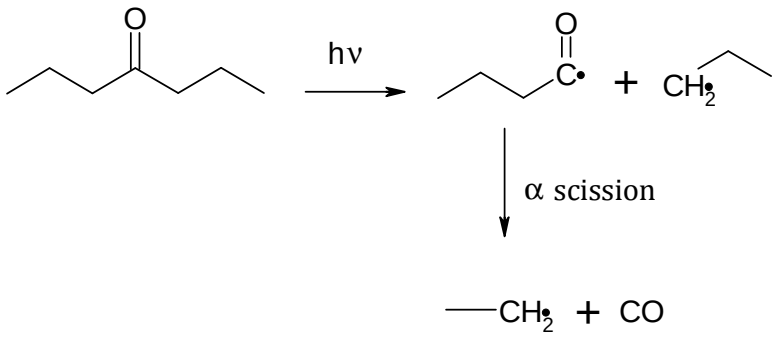

Scheme 1. Formation of carbon monoxide via Norrish I mechanism.

4.2 Temperature effect

Radiation chemical yields for hydrogen and carbon monoxide evolved from polyethylenes irradiated at various temperatures by γ-rays are compiled in Figure 7 (numerical data are given in Table S4 of the Supplementary Information). Dashed lines are added to guide the eye.

To the best of our knowledge, such level off of $G_0(H_2)$ with increasing irradiation temperature has not been described in the literature [12-16]. The authors report the hydrogen emission increasing with temperature ranging from room one to 300 °C, however with different kinetics.

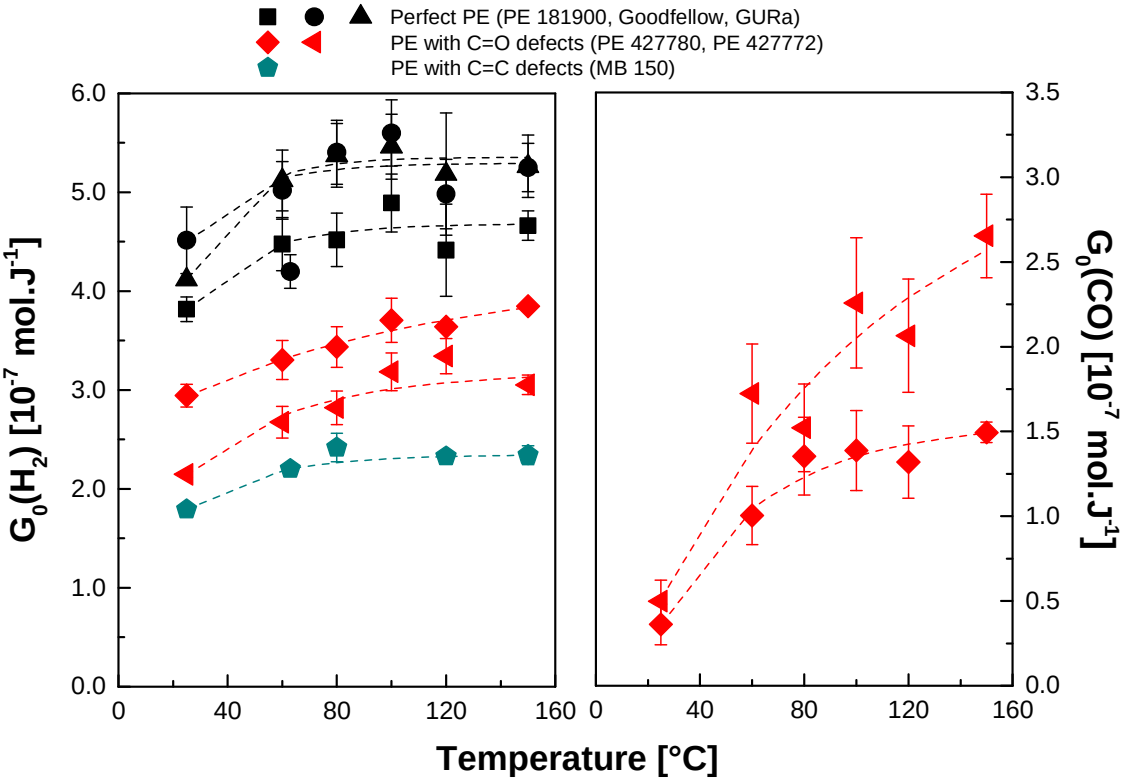

Figure 7. Hydrogen (on the left) and carbon monoxide (on the right) radiation chemical yields as a function of irradiation temperature for different polyethylenes irradiated under helium atmosphere. Dashed lines are added to guide the eye.

As seen in Figure 7, perfect polyethylenes form the highest amount of H_2 by the deposited energy among all tested materials. The distinction in H_2 formation between polyethylenes of different initial composition can be explained by two phenomena. Either the radiation protection effect of double bonds (carbonyl or vinyl) present in polymers is increasing with temperature, or the differences in the degree of crystallinity of the materials can begin to play a role. Nevertheless, as often stated in the literature [6, 20, 29], we believe that the crystallinity will not play a major role, especially above the melting temperature. Hence, we suppose that the radiation protection effect of the two kinds of double bonds under study is at least thermally activated. We note also that the $G_0(H_2)$ value levels off at about 80 °C for all tested materials with the exception of PE 427772 for which it starts to stabilize at around 120 °C. This difference in temperature stabilization demonstrates thus different kinetics of hydrogen formation.

One of the perfect polyethylenes, namely PE 181900, is characterized by lower values of $G_0(H_2)$ in the analyzed range of irradiation temperatures than other ones. As already mentioned in the preceding section, this fact can be explained by the presence of a very low content of effective scavenging vinyls bonds in the chemical structure of this polymer.

Among the materials with confirmed presence of carbonyl defects, PE 427772 is characterized by a lower hydrogen radiation chemical yield than PE 427780, which has previously been explained by its higher ketone bonds concentration. The C=O groups present in polymer backbone become the site of a hydrogen atom abstraction process, leading to the formation of secondary alcohols. This mechanism contributes to the hydrogen radiation chemical yields decrease. This is consistent with the work of Slivinskas *et al.* [9], who studied the effect of ketone polymers on radiation chemical yields and explained the H_2 emission quenching by the intermolecular energy transfer to the carbonyl group along the polymer chain. This mechanism implies the intramolecular charge transfer between neighboring molecules (see Scheme 2 below). In turn, PE 427780 presents a behavior closer to a perfect material, as it contains lower amount of scavenging C=O groups.

The protective role of C=C bonds on the MB150 backbone is also evidenced from Figure 7 [10]. The radiation chemical yields for hydrogen production determined for this material is the lowest one among all the polymers containing double bonds defects in their structure. This observation can come from the difference in their concentration or in a difference in the kind of double bonds efficiency. To differentiate these two hypotheses, the evolution of the relative radiation chemical yields of molecular hydrogen emission at room temperature $\frac{G_0(H_2)_{PE\ with\ defects}}{G_0(H_2)_{Perfect\ PE}}$ as a function of the concentration of chemical defects present in analyzed polyethylenes is depicted in Figure 8, along with the results of Slivinskas *et al*. [9] (ketone groups) and of Ventura *et al.* [10] (*trans*-vinylene groups). The results obtained in this work are in good agreement with those from the literature and confirm that the main influence on hydrogen radiation chemical yield is coming from the concentration of chemical defects, not from their nature.

In Figure 8, the superposition of the curves relative to ketones and *trans*-vinylenes suggests that the mechanism of quenching is the same for both types of defects. It is supposed that part of the energy deposited migrates and is transferred to C=O or C=C groups. Data presented in Figure 8 show that a small concentration of defects reduce significantly hydrogen radiation chemical yields. This result can only be explained by assuming that the excitation can be transferred over large distances, which is reminiscent with the Partridge model [18]. Recent *ab initio* simulations carried out by Ceresoli *et al*. [30] confirmed the rapid migration of exciton along the chain and its trapping by *trans*-vinylene and carbonyl defects. In the same way, Ventura *et al.* [10]

supposed that the energy transfer is possible only in a "sphere of action" around each defects. Then, if the excited molecule is within this sphere, it is fully or partly deactivated. The expression of the relative hydrogen yield is given by equation (2):

$$\frac{G_0(H_2)_C}{G_0(H_2)_{Perfect\ PE}} = \alpha^{ns} + (1 - \alpha^{ns}) \cdot e^{-\nu \cdot N_A \cdot C \cdot \rho} \qquad (2)$$

α^{ns} denotes the non-scavengeable energy fraction, ν corresponds to the "sphere of action" volume in m^3, N_A is the Avogadro number in mol^{-1}, C refers the defects concentration in $mol \cdot kg^{-1}$ and ρ is the density in $kg \cdot mol^{-1}$. For both defects (ketones and *trans*-vinylenes), α^{ns} is comprised between 0.40 and 0.45. This parameter represents either the protection efficiency of the defects or the processes that cannot be scavenged by the defects (non-scavengeable energy).

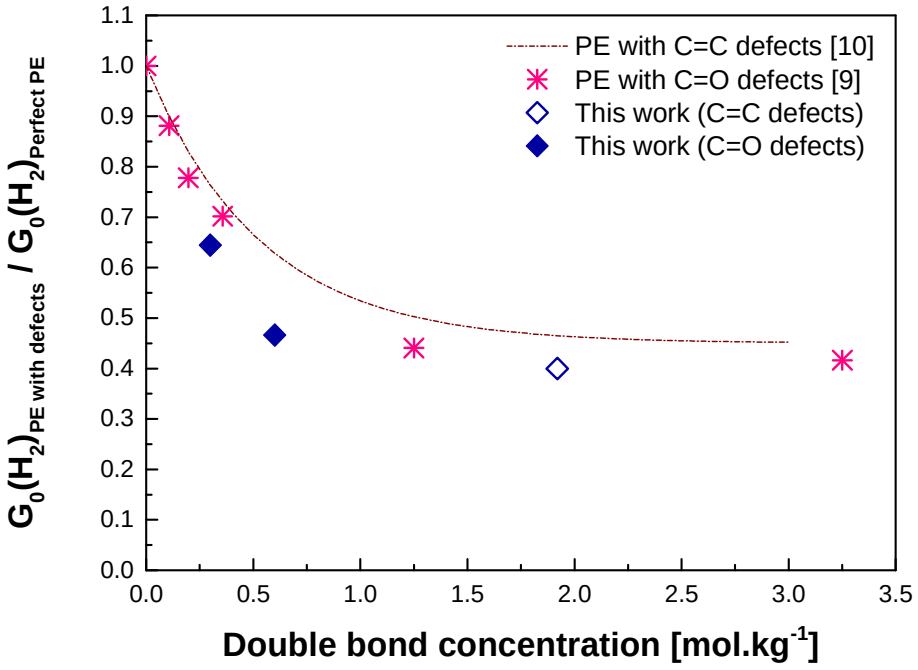

Figure 8: Evolution of relative hydrogen radiation chemical yield of molecular hydrogen emission at room temperature as a function of the concentration of chemical defects (ketones or trans-vinylenes). Results obtained in this work and from the literature [9, 10].

If we consider the temperature effect on hydrogen release presented in Figure 7, then the radiation chemical yields for analyzed perfect polyethylenes increase when the irradiation temperature exceeds the ambient one. At around 100 °C, it starts to stabilize, when taking into account the measurements errors. Very similar dependence is observed for materials containing C=O or C=C defects.

As shown in Figure 8, if the concentration of defects C exceeds 1.5 - 2.0 mol·kg^{-1} then $\frac{G_0(H_2)_C}{G_0(H_2)_{Perfect\ PE}} \approx \alpha^{ns}$. In other words, hydrogen release at room temperature results solely from non-scavengeable energy. If this estimation is used on hydrogen radiation chemical yields obtained for MB150 with the $G_0(H_2)_{Perfect\ PE}(25\,°C)$ used as the reference value, then the following fractions, which are represented in Figure 9, can be calculated:

$$\alpha^{ns}(T) \approx \frac{G_0(H_2)_{MB150}(T)}{G_0(H_2)_{Perfect\ PE}(25\,°C)} \quad \text{and} \quad \alpha^{s}(T) \approx \frac{G_0(H_2)_{Perfect\ PE}(T) - G_0(H_2)_{MB150}(T)}{G_0(H_2)_{Perfect\ PE}(25\,°C)}$$

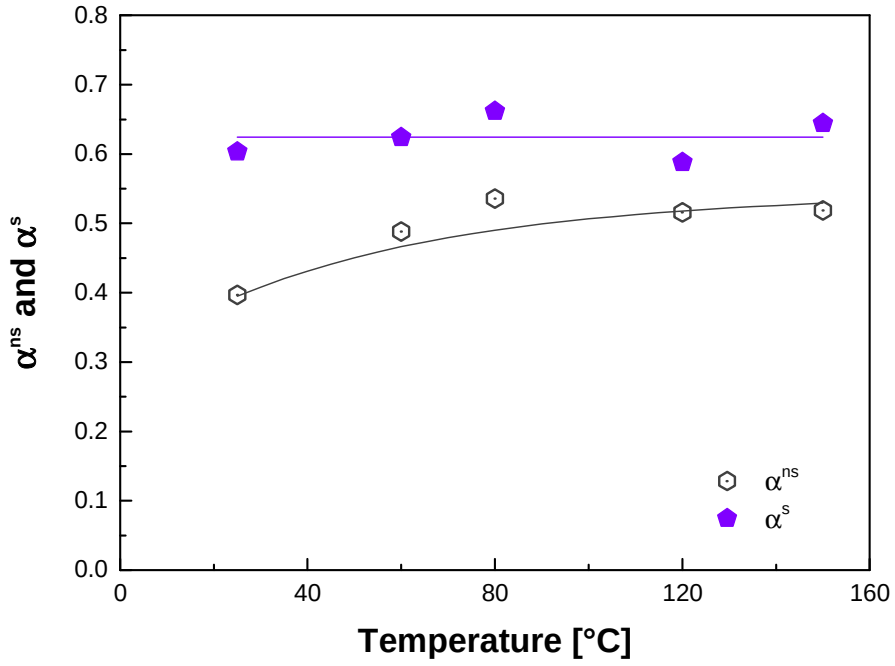

Figure 9: Temperature dependence of the non-scavengeable energy fraction (α^{ns}) and of the scavengeable energy fraction (α^{s}). Results obtained on $G_0(H_2)$ for MB150.

It is evidenced that α^{s}, which designs the scavengeable energy fraction, is roughly constant whatever the irradiation temperature and that the temperature favors the non-scavengeable process. Finally, performed experiments suggest that hydrogen results from at least two distinct mechanisms with different thermal dependence: i) athermal for the scavengeable energy fraction and ii) temperature-dependent for the non-scavengeable energy fraction.

One possible explanation of the α^{ns} apparent increase with the temperature rise is the reduction of the protection efficiency of defects. Nevertheless, this interpretation can be discarded because it is not relevant for polyethylene without defects. The explanation has to be found in primary

mechanism of hydrogen formation. By analogy with alkane radiolysis, hydrogen formation in polyethylene is supposed to result from the decay of excited states and involves the two following mechanisms [31-33]:

- $S_1 \rightarrow S_x$-type internal conversion transitions (IC) that are mainly temperature dependent and lead to H_2 elimination:

$$-CH_2 - CH_2^* - \rightarrow -CH = CH - + H_2$$

- $S_1 \rightarrow T_n$-type intersystem crossing processes (ISC) that are mainly temperature independent and in which triplet state decomposes into radical intermediate products:

$$-CH_2 - CH_2^* - \rightarrow -CH_2 - CH^\circ - + H^\circ$$

$$-CH_2 - CH_2 - + H^\circ \rightarrow -CH_2 - CH^\circ - + H_2$$

The temperature dependence of hydrogen yield is assumed to be due to IC transitions. This interpretation suggests also that the non-scavengeable energy is related to H_2 elimination rather than H atom elimination. According to Partridge [18], this conclusion is problematic as the non-scavengeable energy represents the non-migratory (C-H bond) excitation which is believed to cause C-H bond scission.

Apart from the formation of hydrogen, the emission of carbon monoxide from polyethylenes containing initially carbonyl groups in their polymer backbone is observed. As the C=O repetition units are the sole potential source of carbon monoxide, it can be deduced that carbon monoxide is evolved from the degradation of the polymer specifically localized at the ketone bonds.

Some theoretical *ab initio* simulations were carried out by Ceresoli *et al*. [30] in order to understand the evolution of an exciton trapped on *trans*-vinylene and carbonyl defects which are present in polyethylene. The authors report that excitons trapped by C=O and C=C bonds lead to weakening of these linkages, but without their breaking. However, the researchers do not go so far as to propose a mechanism of ketone cleavage according to the Norrish type I reaction (given on Scheme 1). This reaction involves both the singlet and triplet excited states of ketones and is strongly temperature dependent [34].

In Scheme 2, the excitation transfers and their de-excitation in PE containing C=O is schematically given, along with the direct reaction of hydrogen formation. The two reactions with excitation migration which can be envisaged are thus chain scission and de-excitation without fragmentation. If Scheme 2 is believed to be true, hydrogen and carbon monoxide

formations might be in competition: increase of one gas should imply the decrease of the other one. It is obvious that this is not the case in this work (see Figure 7). It seems therefore that in radiation- and temperature-induced modifications of polyethylenes next to scavenging ISC and non-scavenging IC processes, the third one should probably be considered.

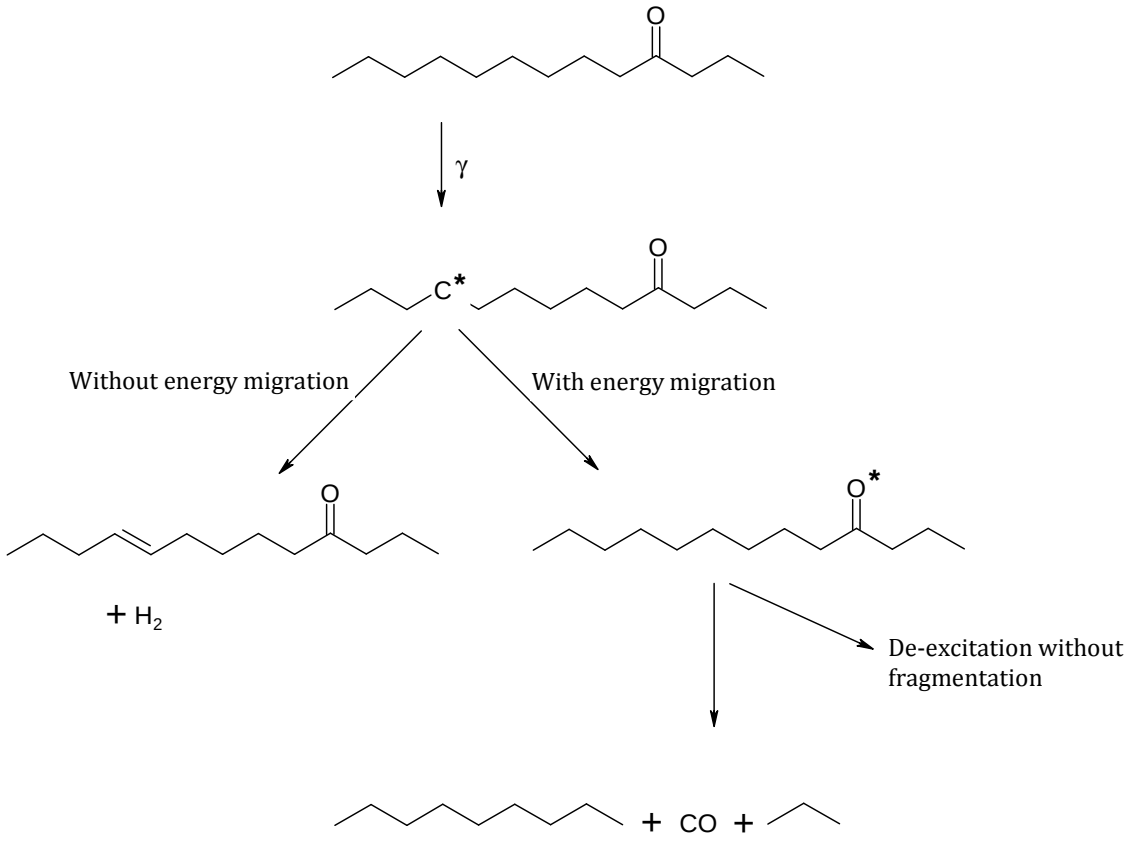

Scheme 2. Possible pathways of de-excitation in polymers containing carbonyl groups.

Conclusions

In order to assess the potential risks in safety management of nuclear packages containing polymers, the potential accumulation of explosive gases during storage, transport and final disposal has to be understood and well evaluated. We have investigated the two following parameters:

- The Linear Energy Transfer (LET) effect by irradiating polymers using γ-rays and SHI,
- The irradiation temperature influence by irradiating polymers using γ-rays at temperatures ranging from room temperature to 150 °C.

We have studied various polyethylenes and methylene based polymers with specific defects (C=C and C=O groups), as these bonds are the main defects formed under irradiation (depending on the atmosphere) and are effective energy and radicals scavengers.

By evaluating the LET effect, it has been shown that hydrogen radiation chemical yields is increasing with the stopping power. It implies that the radiation protection of the defects under study is less effective when LET increases. We have determined the effect of the *trans*-vinylene bonds position (in-chain or on side-chain) at equivalent concentrations and we have observed that the protection is more efficient if the C=C group is located on the backbone. Concentration effect of the double bonds has been determined on the polymers with ketone defects. For these materials, hydrogen radiation chemical yield is decreasing in an equivalent proportion for γ-rays and SHI irradiations: ketone bonds are efficient scavengers and in an equivalent proportion. On the contrary, carbon monoxide released according to the Norrish type I mechanism, is highly dependent on the nature of the irradiation, *i.e.* on the energy and radical transfers.

The efficiency of double bonds is dependent on their concentration in polymer matrix but not on their nature (ketone or *trans*-vinylene bonds). The initial increase of $G_0(H_2)$ with the rise of irradiation temperature was characteristic for all analyzed materials and resulted probably from the growth of polymer chains vibration. By estimating the scavengeable and the non-scavengeable energy fractions, it has been shown that hydrogen results from two distinct mechanisms occurring with different thermal dependence, athermal and temperature-dependent. For polyethylenes containing C=O defects, a schematic reaction mechanism has been proposed. In this process pathway, we suppose the existence of competitive reactions with and without energy migration. Reactions with excitation migration are chain scission and de-excitation without fragmentation.

Finally, it has been demonstrated that whatever the factors under study (LET and irradiation temperature; defects concentration, position and nature), the hydrogen radiation chemical yield

563 is decreased when C=C or C=O bonds are present in the materials. Obtained results are of great
564 significance because of nuclear safety purposes.

565

566 Acknowledgement

567 Authors would like to thank: F. Cochin and F. Nizeyimana (ORANO) for their fruitful discussions;
568 E. Oral (OBBL), M. Bousquié and C. Boisson (LCPP) for supplying samples; P. Le Tutour and P.
569 Quinot (CEA/LABRA) for the gamma irradiations; Y. Ngono-Ravache (CEA/CIMAP) for the ions
570 irradiations; S. Legand (CEA/LRMO) for her help during experiments. This work is financially
571 supported by ORANO and EDF.

572

573 Bibliography

574 [1] Chapiro A. Radiation chemistry of polymeric systems. London: Interscience Publishers; 1962.
575 [2] Dole M, Hedvig P, Humpherys KC, Keyser RM, Mandelkern L, Partridge RH, et al. The
576 radiation chemistry of macromolecules, volume I. London & New York Academic Press Inc.;
577 1972.
578 [3] Ferry M, Ngono-Ravache Y, Aymes-Chodur C, Clochard MC, Coqueret X, Cortella L, et al.
579 Ionizing Radiation Effects in Polymers. Reference Module in Materials Science and Materials
580 Engineering: Elsevier; 2016.
581 [4] Chang Z, LaVerne JA. Hydrogen Production in the Heavy Ion Radiolysis of Polymers. 1.
582 Polyethylene, Polypropylene, Poly(methyl methacrylate), and Polystyrene. J Phys Chem B.
583 2000;104:10557-62.
584 [5] Alexander P, Charlesby A. Radiation protection in copolymers of isobutylene and styrene.
585 Proceedings of the Royal Society of London Series A Mathematical and Physical Sciences.
586 1955;230:136-45.
587 [6] Ferry M, Dannoux-Papin A, Dély N, Legand S, Durand D, Roujou JL, et al. Chemical
588 composition effects of methylene containing polymers on gas emission under γ-irradiation. Nucl
589 Instrum Methods Phys Res, Sect B. 2014;334:69-76.
590 [7] LaVerne JA, Dowling-Medley J. Combinations of Aromatic and Aliphatic Radiolysis. The
591 Journal of Physical Chemistry A. 2015;119:10125-9.
592 [8] Schoepfle CS, Fellows CH. Gaseous Products from Action of Cathode Rays on Hydrocarbons.
593 Industrial & Engineering Chemistry. 1931;23:1396-8.
594 [9] Slivinskas JA, Guillet JE. γ-radiolysis of ketone polymers. III. Copolymers of ethylene and
595 carbon monoxide. Journal of Polymer Science: Polymer Chemistry Edition. 1974;12:1469-91.
596 [10] Ventura A, Ngono-Ravache Y, Marie H, Levavasseur-Marie D, Legay R, Dauvois V, et al.
597 Hydrogen emission and macromolecular radiation-induced defects in polyethylene irradiated
598 under an inert atmosphere: The role of energy transfers toward trans-vinylene unsaturations. J
599 Phys Chem B. 2016;120:10367-80.
600 [11] Arai H, Nagai S, Matsuda K, Hatada M. Effect of irradiation temperature on the radiolysis of
601 methane. Radiation Physics and Chemistry (1977). 1981;17:151-7.
602 [12] Wu G, Katsumura Y, Kudoh H, Morita Y, Seguchi T. Temperature dependence of radiation
603 effects in polyethylene: Cross-linking and gas evolution. Journal of Polymer Science Part A:
604 Polymer Chemistry. 1999;37:1541-8.
605 [13] Seguchi T, Haruyama Y, Sugimoto M. Temperature dependence of gas evolution from
606 polyolefins on irradiation under vacuum. Radiation Physics and Chemistry. 2013;85:124-9.

[14] Mitsui H, Shimizu Y. Kinetic study of the γ radiolysis of polyethylene. Journal of Polymer Science: Polymer Chemistry Edition. 1979;17:2805-13.
[15] Kang HY, Saito O, Dole M. The Radiation Chemistry of Polyethylene. IX. Temperature Coefficient of Cross-Linking and Other Effects. Journal of the American Chemical Society. 1967;89:1980-6.
[16] Bowmer TN, O'Donnell JH. Nature of the side chain branches in low density polyethylene: volatile products from gamma radiolysis. Polymer. 1977;18:1032-40.
[17] Seguchi T. Mechanisms and kinetics of hydrogen yield from polymers by irradiation. Nuclear Instruments and Methods in Physics Research Section B: Beam Interactions with Materials and Atoms. 2001;185:43.
[18] Partridge RH. Excitation Energy Transfer in Alkanes. I. Exciton Model J Chem Phys. 1970;52:2485.
[19] Alexander P, Charlesby A. Energy Transfer in Macromolecules Exposed to Ionizing Radiations. Nature. 1954;173:578.
[20] Williams TF, Dole M. Irradiation of Polyethylene. III. Influence of Temperature and Phase. Journal of American Chemical Society. 1959;81:2919.
[21] Dély N. Radio-oxydation d'un élastomère de type EPDM lors d'irradiations faiblement ou fortement ionisantes : mesure et modélisation de la consommation de dioxygène. Caen: Université de Caen Basse Normandie; 2005.
[22] Ziegler JF. Particle Interactions with Matter. http://www.srim.org/.
[23] George GA, Celina M, Vassallo AM, Cole-Clarke PA. Real-time analysis of the thermal oxidation of polyolefins by FT-IR emission. Polymer Degradation and Stability. 1995;48:199-210.
[24] Gulmine JV, Janissek PR, Heise HM, Akcelrud L. Polyethylene characterization by FTIR. Polymer Testing. 2002;21:557-63.
[25] Colthup NB, Daly LH, Wiberley SE. Introduction to Infrared and Raman Spectroscopy, 3rd ed. Boston: Academic Press, Inc./Harcourt Brace Jovanovich; 1990.
[26] Ferry M, Ngono-Ravache Y, Picq V, Balanzat E. Irradiation of Atactic Polystyrene: Linear Energy Transfer Effects. Journal of Physical Chemistry B. 2008;112:10879.
[27] Geuskens G. Chapter 3 Photodegradation of Polymers. In: Bamford CH, Tipper CFH, editors. Comprehensive Chemical Kinetics: Elsevier; 1975. p. 333-424.
[28] Rabek JF. Photodegradation of polymers: physical characteristics and applications. Berlin: Springer Science & Business Media; 1996.
[29] Kornacka EM, Przybytniak G, Święszkowski W. The influence of crystallinity on radiation stability of UHMWPE. Radiation Physics and Chemistry. 2013;84:151-6.
[30] Ceresoli D, Tosatti E, Scandolo S, Santoro G, Serra S. Trapping of excitons at chemical defects in polyethylene. The Journal of Chemical Physics. 2004;121:6478-84.
[31] Wojnárovits L, Luthjens LH, De Leng HC, Hummel A. On the mechanism of alkane S1 decay. Journal of Radioanalytical and Nuclear Chemistry. 1986;101:349-57.
[32] Wojnarovits L. Photochemistry and Radiation Chemistry of Liquid Alkanes: Formation and Decay of Low-Energy Excited States. In: Mozumder A, Hatano Y, editors. Charged Particle and Photon Interactions with Matter. Boca Raton: CRC Press; 2004. p. 365-402.
[33] Dellonte S, Flamigni L, Barigelletti F, Wojnarovits L, Orlandi G. Temperature dependence of the fluorescence lifetimes of linear alkanes: a correlation with the photodecomposition. The Journal of Physical Chemistry. 1984;88:58-61.
[34] Hartley GH, Guillet JE. Photochemistry of Ketone Polymers. I. Studies of Ethylene-Carbon Monoxide Copolymers. Macromolecules. 1968;1:165-70.